

# Pt-Rh/CeO<sub>2</sub>-Al<sub>2</sub>O<sub>3</sub> for Controlling Emissions from Natural Gas Engines: Three-Way Catalytic Activity at Low Temperatures and Effects of SO<sub>2</sub> Aging

Hirofumi Ohtsuka

Received: 19 November 2014 / Revised: 8 December 2014 / Accepted: 10 December 2014  
© Springer SIP, AG 2014

**Abstract** The three-way catalytic activity of Pt-Rh/CeO<sub>2</sub>-Al<sub>2</sub>O<sub>3</sub> was examined at temperatures below 500 °C under conditions simulating gas engine exhaust, and the results were compared with those of O<sub>2</sub>-CH<sub>4</sub>, NO-O<sub>2</sub>-CH<sub>4</sub>, and NO-CH<sub>4</sub> model reactions. The catalyst exhibited sufficient three-way catalytic activity, even at 400 °C, in the absence of SO<sub>2</sub>. After SO<sub>2</sub> aging, the activity under stoichiometric conditions remarkably decreased. In addition, methane conversion under rich (reducing) conditions severely decreased after SO<sub>2</sub> aging due to the suppression of steam methane reforming by sulfur poisoning.

**Keywords** Three-way catalyst (TWC) · Natural gas vehicle (NGV) · Platinum · Rhodium · Methane

## 1 Introduction

Among fossil fuels, natural gas produces the least carbon dioxide per unit of energy and is thus the most favorable in terms of environmental impact [1]. Recent advances in shale gas exploitation have significantly increased the supply of natural gas and stabilized the price of natural gas, increasing its attractiveness as a fuel [2]. Internal combustion engines fuelled by natural gas are widely used in natural gas vehicles (NGV), combined heat and power (CHP) plants, and gas engine-driven heat pump units (GHP). To control emissions from these engines, three-way catalyst systems similar to those used in gasoline-fuelled vehicles are widely applied. However, in contrast to gasoline engine exhaust, which contains a large amount of reactive hydrocarbons such as C<sub>2</sub>H<sub>4</sub>

and C<sub>3</sub>H<sub>6</sub>, the main hydrocarbon component in gas engine exhaust is methane [3]. Because methane is the least reactive hydrocarbon, obtaining a high methane conversion at low temperatures is the principal issue in controlling emissions from natural gas engines by three-way catalysts [4–6].

A Pt-Rh/CeO<sub>2</sub>-Al<sub>2</sub>O<sub>3</sub> catalyst with high Pt loading has been developed as a catalyst that exhibits high durability under the conditions of emission control from gas engines, with a reported long-term durability of more than 30,000 h [7–9]. However, with growing concerns about global warming and concomitant tightening of fuel efficiency regulations, further increases in the efficiencies of gas engines are sought, and efficiency improvement measures such as exhaust gas recirculation (EGR) are being intensively studied. Improvements in fuel efficiency inevitably cause a decrease in the exhaust temperature. This imposes a further challenge for controlling emissions from natural gas engines. The selective catalytic reduction of NO<sub>x</sub> with methane (CH<sub>4</sub>-SCR) coupled with lean combustion can be an alternative solution and has been studied extensively [10–15]. However, activities of the reported catalysts are not sufficient to obtain NO<sub>x</sub> and CH<sub>4</sub> conversions required in practical applications.

A number of studies have examined three-way catalysts for natural gas engines and related reactions. Subramanian and coworkers extensively investigated model reactions (CH<sub>4</sub>-NO-CO-H<sub>2</sub>-O<sub>2</sub>, CH<sub>4</sub>-NO-CO-O<sub>2</sub>, CH<sub>4</sub>-O<sub>2</sub>, CH<sub>4</sub>-NO, etc.) over 1 % Pd/Al<sub>2</sub>O<sub>3</sub> with different feedstream compositions, from reducing to stoichiometric to oxidizing atmospheres [16]. However, the temperature examined in their study was limited to 550 °C, and activity at lower temperatures was not examined. Oh and coworkers investigated methane oxidation over noble metal (Pt, Pd, Rh) catalysts supported on Al<sub>2</sub>O<sub>3</sub> and CeO<sub>2</sub>/Al<sub>2</sub>O<sub>3</sub> with varying oxygen concentrations between 0.2 and 1 % [17, 18]. They observed that methane conversion was maximal at approximately stoichiometric oxygen concentrations and decreased under oxidizing conditions, concluding

H. Ohtsuka (✉)  
Energy Technology Laboratories, Osaka Gas Co., Ltd.,  
6-19-9 Torishima, Konohana-ku, Osaka 554-0051, Japan  
e-mail: ohtsuka@osakagas.co.jp

that the decrease in methane conversion under oxidizing conditions was due to strong adsorption of oxygen on the surface of the noble metals comprising the active sites. Burch and Ramli investigated NO reduction by CH<sub>4</sub> over Pt, Pd, and Rh catalysts supported on SiO<sub>2</sub> and Al<sub>2</sub>O<sub>3</sub> [19, 20]. They determined that Pt had the highest activity, which was an order of magnitude higher than those of Pd and Rh. It was suggested that the relative activities of the catalysts reflected the ease of reduction of the catalysts. González-Velasco and coworkers investigated three-way catalytic reactions over Pt/Al<sub>2</sub>O<sub>3</sub> in the presence of H<sub>2</sub>O (10 %) and CO<sub>2</sub> (10 %), which are present in actual engine exhaust [21]. In a comparison of CH<sub>4</sub>, C<sub>2</sub>H<sub>4</sub>, C<sub>3</sub>H<sub>6</sub>, and C<sub>4</sub>H<sub>8</sub> as the hydrocarbon components, they demonstrated that a high hydrocarbon conversion of ca. 100 % was obtained under net oxidizing conditions when hydrocarbons other than CH<sub>4</sub> were used, while CH<sub>4</sub> conversion was very low except under slightly reducing conditions.

In this work, the three-way catalytic activity of a Pt-Rh/CeO<sub>2</sub>-Al<sub>2</sub>O<sub>3</sub> catalyst that is widely used in natural gas engines was investigated at relatively low temperatures (400–500 °C) under conditions simulating natural gas engine exhaust. The effects of S poisoning, which are expected to be severe at lower temperatures, were also examined.

## 2 Experimental

### 2.1 Catalyst Preparation

Commercial  $\gamma$ -Al<sub>2</sub>O<sub>3</sub> (4- to 6-mm spheres, Kishida Chemical, Osaka) was crushed and sieved to 1- to 2-mm grains, which were impregnated with Ce (10 wt%) using an aqueous solution of cerium nitrate (Ce(NO<sub>3</sub>)<sub>3</sub>·6H<sub>2</sub>O, Mitsuwa Chemicals, Osaka), followed by drying at 120 °C and calcining in air at 700 °C for 6 h to obtain a CeO<sub>2</sub>-Al<sub>2</sub>O<sub>3</sub> support.

The support was loaded with Pt (2.0 wt%) and Rh (0.2 wt%) by impregnation using Pt(NO<sub>2</sub>)<sub>2</sub>(NH<sub>3</sub>)<sub>2</sub> (Kojima Chemicals, Tokyo) and Rh(NO<sub>3</sub>)<sub>3</sub> (N.E. Chemcat, Tokyo) as precursors. The impregnated solid was dried at 120 °C and calcined in air at 550 °C for 6 h to obtain the Pt-Rh/CeO<sub>2</sub>-Al<sub>2</sub>O<sub>3</sub> catalyst.

### 2.2 Catalytic Activity Measurements

Catalytic activity was measured using a fixed-bed flow reactor. The catalyst grains (1.45 g, ca. 1.9 mL) were placed in a quartz tube (inside diameter 14 mm, length 740 mm) and heated with an electric furnace (ARF3-500, Asahi Rika, Chiba, Japan). The temperature of the catalyst bed was measured with a thermocouple inserted into the quartz tube. The reaction gas was prepared by mixing 5000 ppm NO/He, 3 % CH<sub>4</sub>/He, 2 % CO, 1.2 % H<sub>2</sub>/He, 30 ppm SO<sub>2</sub>/He, O<sub>2</sub> (99.97 %, Takachiho Chemical, Tokyo), CO<sub>2</sub> (99.999 %, Takachiho

Chemical), and He (99.999 %, Iwatani Industrial Gases, Osaka) gases using mass flow controllers (HM5141B, Hemmi Slide Rule, Tokyo). Water vapor was introduced by passing a portion of the helium through a water saturator. The gas flow rate was 1.675 L/min, which corresponded to a gas hourly space volume (GHSV) of 53,000/h.

The feedstream compositions shown in Table 1 were used in the experiments under simulated gas engine exhaust conditions. The compositions were similar to those of actual gas engine exhaust, except the concentrations of CO<sub>2</sub> and H<sub>2</sub>O, which were reduced for experimental accuracy. The O<sub>2</sub>-CH<sub>4</sub>, NO-O<sub>2</sub>-CH<sub>4</sub>, and NO-CH<sub>4</sub> reactions were also examined as model reactions for three-way catalytic reactions. All activity measurements were performed under a range of conditions from rich (reducing) conditions to lean (oxidizing). For activity measurements of model reactions, pretreatment with a gas containing 3000 ppm CO, 1800 ppm H<sub>2</sub>, and 5 % H<sub>2</sub>O in He for 10 min was conducted before measurements at each temperature.

The feedstream composition was maintained constant for 25 min before the effluent gas was analyzed. A pair of chemiluminescence NO<sub>x</sub> analyzers (ECL-88A Lite, Anatec Yanaco, Kyoto) was used to measure NO<sub>x</sub> concentrations. The NO<sub>x</sub> concentration is the sum of the NO and NO<sub>2</sub> concentrations, and the NO<sub>x</sub> conversion ( $X_{\text{NO}}$ ) is calculated by the following equation, where the suffixes “in” and “out” indicate the concentrations at the inlet and outlet of the reactor, respectively.

$$X_{\text{NO}}(\%) = 100 \times \left\{ 1 - \frac{([\text{NO}]_{\text{out}} + [\text{NO}_2]_{\text{out}})}{([\text{NO}]_{\text{in}} + [\text{NO}_2]_{\text{in}})} \right\}$$

The concentrations of H<sub>2</sub>, CO, CO<sub>2</sub>, CH<sub>4</sub>, O<sub>2</sub>, and N<sub>2</sub>O were measured by gas chromatography (GC-2014ATF and GC-8AIT, Shimadzu, Kyoto). Hydrogen was separated using a MS-13X column (16 m); O<sub>2</sub>, N<sub>2</sub>, and CO were separated using a MS-5A column (2 m); and CO<sub>2</sub> and N<sub>2</sub>O were separated using a Gaskuropack 54 (4 m, GL Sciences, Tokyo). The concentration of each component was measured using a

**Table 1** Feedstream compositions for activity measurements under conditions simulating gas engine exhaust. Concentrations of other components were maintained constant: CH<sub>4</sub> 1500 ppm, CO<sub>2</sub> 6 %, H<sub>2</sub>O 11 %

$\lambda$	NO (ppm)	O <sub>2</sub> (ppm)	CO (ppm)	H <sub>2</sub> (ppm)
0.985	1400	3440	5000	3000
0.990	1600	3650	4200	2520
0.995	1800	3870	3400	2040
0.998	1920	3990	2920	1750
0.999	1960	4040	2760	1660
1.000	2000	4080	2600	1560
1.002	2080	4170	2280	1370
1.005	2200	4300	1800	1080

thermal conductivity detector (TCD). Methane was separated using a Gaskuropack 54 (2 m) and measured with a flame ionization detector (FID). The minimum detectable concentrations for gas chromatography were approximately 40 ppm for O<sub>2</sub>, CO, CO<sub>2</sub>, and N<sub>2</sub>O; 200 ppm for H<sub>2</sub>; and 5 ppm for CH<sub>4</sub>.

In experiments under simulated exhaust conditions, catalytic activity was measured from 550 to 400 °C in intervals of 25 °C. After measurements at 400 °C, the catalyst was subjected to SO<sub>2</sub> aging by introducing a gas with a composition of 100 ppm NO, 1000 ppm CO, 600 ppm H<sub>2</sub>, 3 ppm SO<sub>2</sub>, 1500 ppm CH<sub>4</sub>, 5 % O<sub>2</sub>, 6 % CO<sub>2</sub>, and 11 % H<sub>2</sub>O balanced with He for 18 h (flow rate 1.675 L/min) while the temperature of the catalyst bed was maintained at 400 °C. The activity of the aged catalyst was measured from 400 to 550 °C in intervals of 25 °C. The catalytic activity in the model reactions was measured at 500 °C followed by 450 and 400 °C for the fresh catalyst and at 400 °C followed by 450 and 500 °C for the SO<sub>2</sub>-aged catalyst. During activity measurements after SO<sub>2</sub> aging, 1 ppm SO<sub>2</sub> was added to the feedstream to avoid de poisoning of the catalyst.

To compare conversions under simulated exhaust conditions with those of the model reactions, the conversions were plotted against the air to fuel equivalence ratio ( $\lambda$ ), which is widely used as a parameter for controlling internal combustion engines. The air to fuel equivalence ratio ( $\lambda$ ) is defined as the ratio of the actual amount of air introduced into the combustion chamber to the amount of air that is required to completely combust the fuel. When the only exhaust hydrocarbon is CH<sub>4</sub>,  $\lambda$  is calculated according to the following equation [5], where the concentrations (ppm) of the species are in brackets.

$$\lambda = 1 + ([\text{O}_2] + 0.5[\text{NO}] - 0.5[\text{H}_2] - 0.5[\text{CO}] - 2[\text{CH}_4]) / (1.91 \times 10^5)$$

### 2.3 Characterization

Specific surface area measurements were obtained with an automatic surface area analyzer (AMS-8000, Ohkura Riken, Tokyo). The adsorption of N<sub>2</sub> was measured at 77 K and  $P/P_0=0.3$ , and the Brunauer-Emmett-Teller (BET) surface area was calculated according to the one-point method. Measurements of CO adsorption were conducted using a pulsed-flow adsorption analyzer (R-6015, Ohkura Riken). Samples were pretreated under a H<sub>2</sub> flow at 200 °C for 30 min, and the adsorption of CO was measured at 50 °C.

Powder X-ray diffraction patterns were measured using Cu K $\alpha$  radiation on an X-ray diffractometer equipped with a graphite monochromator (XRD-6100, Shimadzu). The X-ray tube (PW2233/20, PANalytical) was operated at 40 kV and a current of 40 mA. The patterns were recorded over a  $2\theta$  range of 20° to 74° with a step size of 0.02°, a dwell time of 1.2 s, and a rotation speed of 50 rpm.

### 3 Results

Figure 1 shows the X-ray diffractograms of the support and the catalyst. In the X-ray diffractogram of the support, diffraction lines for CeO<sub>2</sub> at 28.6°, 33.1°, 47.5°, and 56.3° and for Al<sub>2</sub>O<sub>3</sub> at ca. 67° were observed. No appreciable changes in these diffraction lines were observed after loading Pt-Rh or after activity measurements. Table 2 shows the BET specific surface areas and CO adsorption results. The changes in the BET surface areas were also small. These results suggest that the support itself was not essentially affected by the loading of Pt-Rh or the activity measurements. In the X-ray diffractogram of the catalyst, a broad diffraction line for metallic Pt was observed at ca. 40°. The intensity of this line increased after activity measurements, suggesting that the supported Pt agglomerated to form metallic Pt particles under the reaction conditions. A significant decrease in the amount of CO adsorbed was observed after activity measurements. The catalysts exhibited a larger decrease in the amount of CO adsorbed after SO<sub>2</sub> aging, which may indicate that sulfur promoted Pt agglomeration, but the adsorbed sulfur species that remained after pretreatment may have inhibited the adsorption of CO, reducing the amount of CO adsorption on the SO<sub>2</sub>-aged catalysts.

Figure 2 shows the NO<sub>x</sub>, CO, and CH<sub>4</sub> conversions under conditions simulating gas engine exhaust. Over the fresh (before SO<sub>2</sub> aging) catalyst at 550 °C, all of the NO<sub>x</sub>, CO, and CH<sub>4</sub> conversions exceeded 99 % under stoichiometric conditions ( $\lambda=1.000$ ). Under rich conditions ( $\lambda<1.000$ ), CO conversion decreased, but high CH<sub>4</sub> conversion was maintained. By contrast, under lean conditions ( $\lambda>1.000$ ), NO<sub>x</sub> conversion sharply decreased, with an increase in  $\lambda$  accompanied by a slight decrease in CH<sub>4</sub> conversion. As the reaction temperature decreased, the NO<sub>x</sub> and CH<sub>4</sub> conversions

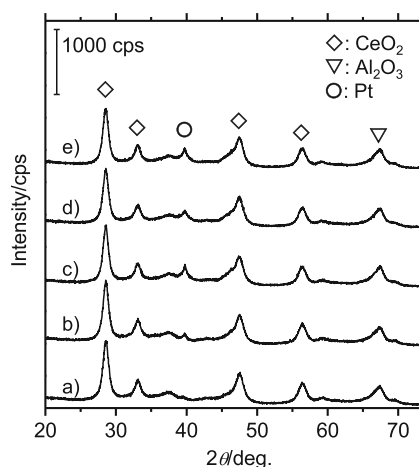


**Fig. 1** X-ray diffractogram of the support and catalyst. a) CeO<sub>2</sub>-Al<sub>2</sub>O<sub>3</sub>, b) Pt-Rh/CeO<sub>2</sub>-Al<sub>2</sub>O<sub>3</sub>, c) Pt-Rh/CeO<sub>2</sub>-Al<sub>2</sub>O<sub>3</sub> after reaction under simulated gas engine exhaust conditions, d) Pt-Rh/CeO<sub>2</sub>-Al<sub>2</sub>O<sub>3</sub> after reaction under model gas conditions without S aging, and e) Pt-Rh/CeO<sub>2</sub>-Al<sub>2</sub>O<sub>3</sub> after reaction under model gas conditions with S aging

**Table 2** BET surface areas and amounts of CO adsorption on the support and catalysts

	BET surface area (m <sup>2</sup> /g)	CO adsorption (mL/g)
CeO <sub>2</sub> -Al <sub>2</sub> O <sub>3</sub>	109	— <sup>a</sup>
Pt-Rh/CeO <sub>2</sub> -Al <sub>2</sub> O <sub>3</sub>		
As prepared	106	1.09
After activity measurements		
Under simulated exhaust	102	0.242
Under model reactions without S aging	105	0.466
Under model reactions with S aging	105	0.281

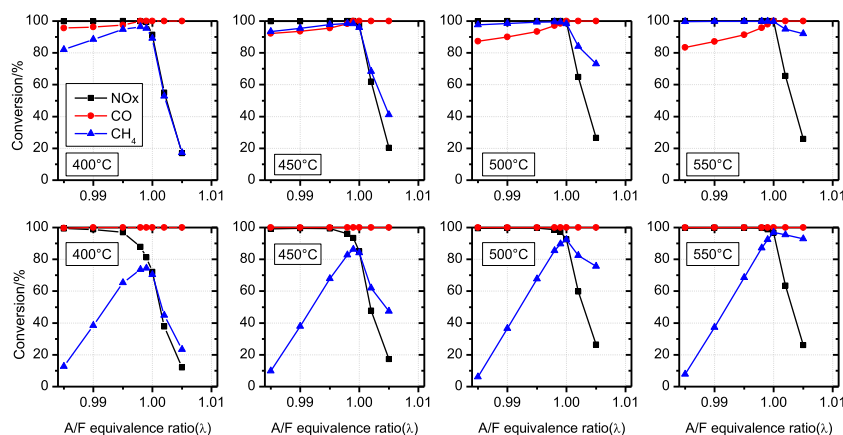
<sup>a</sup> Not measured

decreased under stoichiometric conditions ( $\lambda=1.000$ ), with NO<sub>x</sub> and CH<sub>4</sub> conversions at 400 °C of 91 and 89 %, respectively. CH<sub>4</sub> conversion under lean conditions decreased remarkably at lower temperatures, and CH<sub>4</sub> conversion also decreased under rich conditions. Concomitant with the decrease in CH<sub>4</sub> conversion under rich conditions, the CO conversion under rich conditions increased. That is, when components in the effluent gas were compared at the same  $\lambda$ , the concentration of CH<sub>4</sub> increased and the concentrations of CO and H<sub>2</sub> decreased. At all temperatures between 400 and 550 °C, the reaction effluent contained H<sub>2</sub> at a concentration of 4000–6000 ppm at  $\lambda=0.985$ , higher than the H<sub>2</sub> concentration in the feedstream. These results suggest that H<sub>2</sub> was formed by steam reforming of CH<sub>4</sub>. The concentration ratio of H<sub>2</sub>/CO was 5.9 (550 °C)–17 (400 °C), which is nearly identical to the ratio in the chemical equilibrium of the water-gas shift reaction (6.1 [550 °C]–21 [400 °C]). The effect of SO<sub>2</sub> aging on NO<sub>x</sub> and CH<sub>4</sub> conversion was remarkable at 500 °C and lower temperatures under stoichiometric conditions ( $\lambda=1.000$ ). After SO<sub>2</sub> aging, NO<sub>x</sub> and CH<sub>4</sub> conversions decreased to 72 and 70 %, respectively, at 400 °C. While the CH<sub>4</sub> conversion under rich conditions remarkably decreased after SO<sub>2</sub> aging, the CH<sub>4</sub> conversion under lean conditions was affected very little or slightly increased. The effluent from the

aged catalyst under rich conditions contained almost solely CH<sub>4</sub> as the reducing component, while the concentrations of H<sub>2</sub> and CO were very low or below the detection limits. The conversion of CH<sub>4</sub> at  $\lambda=0.985$ –0.995 did not change appreciably with the reaction temperature, most likely because CH<sub>4</sub> conversion was determined by the feedstream composition and not the reaction rate. In fact, under conditions of  $\lambda=0.985$ –0.995, the NO<sub>x</sub> and O<sub>2</sub> conversions were ca. 100 % between 400 and 550 °C, and the observed CH<sub>4</sub> conversion corresponded to the calculated CH<sub>4</sub> conversion under the assumption that excess reducing components exit the reactor as methane (5, 36, and 68 % for  $\lambda=0.985$ , 0.990, and 0.995, respectively).

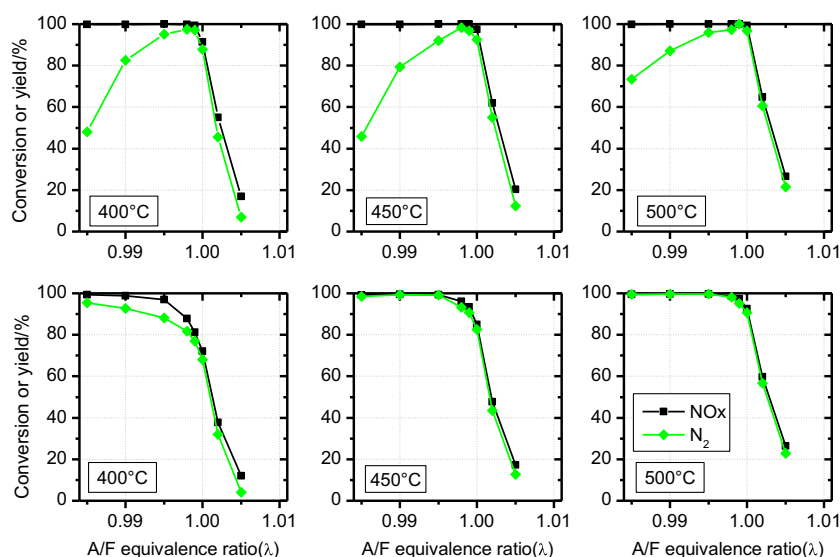
Figure 3 shows the N<sub>2</sub> yield from the activity measurements shown in Fig. 2. Over the fresh catalyst, the N<sub>2</sub> yield was in good agreement with the NO conversion under stoichiometric to lean conditions, which indicates that NO was converted to N<sub>2</sub> with high selectivity. By contrast, under rich conditions, the N<sub>2</sub> yield decreased significantly with decreasing  $\lambda$ . Under the experimental conditions, the large amount of CO<sub>2</sub> contained in the feedstream prevented precise determination of the effluent N<sub>2</sub>O concentration, but formation of a large amount of N<sub>2</sub>O can be ruled out. Therefore, NO that was not converted to N<sub>2</sub> most likely formed NH<sub>3</sub>. After SO<sub>2</sub> aging, a decrease in the N<sub>2</sub> yield under rich conditions was not observed, and at 450 °C or higher, the N<sub>2</sub> yield was in good agreement with the NO conversion throughout the entire  $\lambda$  range examined. As mentioned above, the reaction effluent contained large amounts of H<sub>2</sub> before SO<sub>2</sub> aging but only small amounts of H<sub>2</sub> after SO<sub>2</sub> aging. Large amounts of NH<sub>3</sub> are formed in the NO-H<sub>2</sub> reaction over Pt catalysts under H<sub>2</sub>-rich conditions [22]; the suppression of the formation of H<sub>2</sub>, which is required to form NH<sub>3</sub>, is likely responsible for the suppression of NH<sub>3</sub> formation after SO<sub>2</sub> aging.

Figure 4 shows the CH<sub>4</sub> conversion in the activity measurements under the simulated exhaust conditions as a function of temperature. Over the fresh catalyst, the CH<sub>4</sub> conversion at  $\lambda=0.985$  was 82 % at 400 °C and increased with increasing reaction temperature, reaching 98 % at 500 °C.

**Fig. 2** NO<sub>x</sub>, CO, and CH<sub>4</sub> conversions over Pt-Rh/CeO<sub>2</sub>-Al<sub>2</sub>O<sub>3</sub> under gas engine exhaust conditions before (*upper column*) and after (*lower column*) S aging



**Fig. 3**  $\text{NO}_x$  conversions and  $\text{N}_2$  yields over Pt-Rh/CeO<sub>2</sub>-Al<sub>2</sub>O<sub>3</sub> under gas engine exhaust conditions before (*upper column*) and after (*lower column*) S aging



Under lean conditions ( $\lambda=1.005$ ), the  $\text{CH}_4$  conversion was 17 % at 400 °C, considerably lower than that under rich conditions.  $\text{CH}_4$  conversion under lean conditions also increased with increasing reaction temperature but reached only 73 % at 500 °C and 92 % at 550 °C. The effects of  $\text{SO}_2$  aging on  $\text{CH}_4$  conversion were remarkably different under rich or lean conditions. Under lean conditions,  $\text{SO}_2$  aging did not affect or slightly promoted  $\text{CH}_4$  conversion. By contrast,  $\text{SO}_2$  aging drastically suppressed  $\text{CH}_4$  conversion under rich conditions.  $\text{CH}_4$  conversion after  $\text{SO}_2$  aging exhibited a maximum at 425 °C and decreased with increasing temperature up to 500 °C.

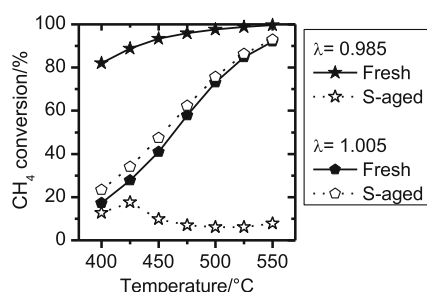
Figure 5 shows the  $\text{CH}_4$  conversion in the  $\text{O}_2$ - $\text{CH}_4$  reaction. Before  $\text{SO}_2$  aging, a high  $\text{CH}_4$  conversion was observed under stoichiometric and rich conditions. At  $\lambda=1.000$ , the  $\text{CH}_4$  conversion was 91 % at 400 °C and ca. 100 % at 500 °C. At  $\lambda=0.984$ , the  $\text{CH}_4$  conversion was 84 % at 400 °C and ca. 100 % at 500 °C. By contrast, under lean conditions, the  $\text{CH}_4$  conversion decreased with increasing  $\lambda$ . At 400 °C, the  $\text{CH}_4$  conversion fell to 16 % at  $\lambda=1.010$ . The feedstream composition at  $\lambda=0.984$  was 1500 ppm  $\text{CH}_4$  and 11 %  $\text{H}_2\text{O}$  balanced with He. Obviously, the  $\text{CH}_4$  was converted solely by steam reforming under this condition, as demonstrated by  $\text{H}_2$  formation. The reaction

effluent contained ca. 6000 ppm  $\text{H}_2$  at 500 °C and ca. 5000 ppm  $\text{H}_2$  at 400 °C, in agreement with the calculated  $\text{H}_2$  concentrations assuming steam reforming and water-gas shift reactions ( $\text{H}_2$  4 mol/mol- $\text{CH}_4$ ). In the presence of  $\text{O}_2$ , the concentration of  $\text{H}_2$  decreased, but  $\text{H}_2$  formation was still observed (ca. 2000 ppm  $\text{H}_2$  at 500 °C and  $\lambda=0.995$ , i.e.,  $\text{CH}_4$  1500 ppm,  $\text{O}_2$  2000 ppm, 11 %  $\text{H}_2\text{O}$ ).

The effects of  $\text{SO}_2$  aging on  $\text{CH}_4$  conversion in the  $\text{O}_2$ - $\text{CH}_4$  reaction differed substantially under rich or lean conditions. Under rich conditions,  $\text{CH}_4$  conversion was drastically suppressed, and  $\text{H}_2$  formation became insignificant after  $\text{SO}_2$  aging, indicating nearly complete suppression of steam reforming of  $\text{CH}_4$ . By contrast,  $\text{SO}_2$  aging did not significantly affect  $\text{CH}_4$  conversion under lean conditions. The  $\text{CH}_4$  conversion characteristics and the effects of  $\text{SO}_2$  aging in the  $\text{O}_2$ - $\text{CH}_4$  reaction resembled those under simulated exhaust conditions.

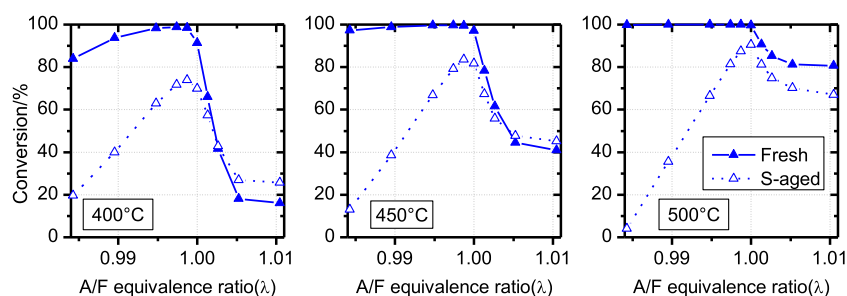
Figure 6 shows the  $\text{NO}_x$  and  $\text{CH}_4$  conversions in the  $\text{NO}$ - $\text{O}_2$ - $\text{CH}_4$  reaction. Over the fresh catalyst, a  $\text{NO}_x$  conversion of 93 % and a  $\text{CH}_4$  conversion of 93 % were obtained under stoichiometric conditions (2000 ppm  $\text{NO}$ , 2000 ppm  $\text{O}_2$ , 1500 ppm  $\text{CH}_4$ ) at 400 °C, in good agreement with the  $\text{NO}_x$  and  $\text{CH}_4$  conversions under simulated exhaust conditions (91 and 89 %, respectively). After  $\text{SO}_2$  aging, the  $\text{NO}_x$  and  $\text{CH}_4$  conversions in the  $\text{NO}$ - $\text{O}_2$ - $\text{CH}_4$  reaction were also similar to those under simulated exhaust conditions.

Figure 7 shows the  $\text{N}_2$  and  $\text{N}_2\text{O}$  yields in the  $\text{NO}$ - $\text{O}_2$ - $\text{CH}_4$  reaction. Over the fresh catalyst, the  $\text{N}_2$  yield was in good agreement with the  $\text{NO}_x$  conversion under stoichiometric to lean conditions but decreased with decreasing  $\lambda$  under rich conditions. Because  $\text{N}_2\text{O}$  was not observed in the effluent under rich conditions, the  $\text{NO}_x$  that did not form  $\text{N}_2$  was likely converted to  $\text{NH}_3$ . After  $\text{SO}_2$  aging,  $\text{N}_2\text{O}$  formation was observed at 400 °C,  $\lambda=0.995$  ( $\text{N}_2\text{O}$  yield 7 %), but the  $\text{N}_2$



**Fig. 4**  $\text{CH}_4$  conversions over Pt-Rh/CeO<sub>2</sub>-Al<sub>2</sub>O<sub>3</sub> as a function of temperature under gas engine exhaust conditions

**Fig. 5** CH<sub>4</sub> conversions over Pt-Rh/CeO<sub>2</sub>-Al<sub>2</sub>O<sub>3</sub> in the O<sub>2</sub>-CH<sub>4</sub> reaction. Reaction conditions: 1500 ppm CH<sub>4</sub>, 0–5000 ppm O<sub>2</sub>, 11 % H<sub>2</sub>O

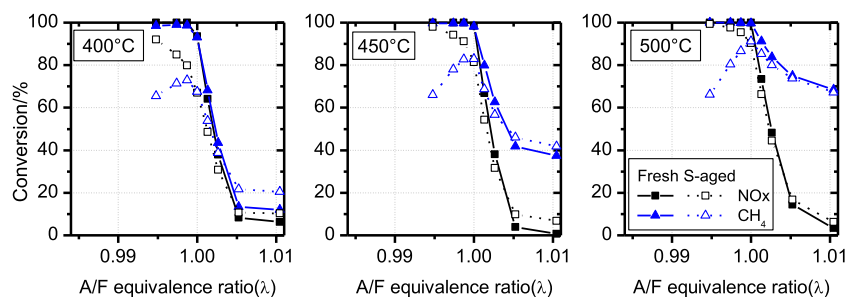


yield was otherwise nearly in agreement with the NO<sub>x</sub> conversion. Similar to the results obtained under simulated exhaust conditions, the effluent from the fresh catalyst contained H<sub>2</sub> under rich conditions, with a H<sub>2</sub> concentration of ca. 2000 ppm at λ=0.995. These results indicate that the NO<sub>x</sub> and CH<sub>4</sub> conversions and the N<sub>2</sub> yield in the NO-O<sub>2</sub>-CH<sub>4</sub> reaction are in good agreement with those obtained under simulated exhaust conditions.

Figure 8 shows the NO<sub>x</sub> and CH<sub>4</sub> conversions in the NO-CH<sub>4</sub> reaction. At 400 °C, λ=1.000, the NO<sub>x</sub> conversion was 99.7 % over the fresh catalyst and 96 % over the SO<sub>2</sub>-aged catalyst. At 450 and 500 °C, the NO<sub>x</sub> conversion at λ=1.000 was ca. 100 % over both of the fresh catalyst and the SO<sub>2</sub>-aged catalyst. These conversions are remarkably higher than those observed under simulated exhaust conditions or in the NO-O<sub>2</sub>-CH<sub>4</sub> reaction. However, the NO<sub>x</sub> and CH<sub>4</sub> conversions decreased under lean conditions. Under rich conditions, H<sub>2</sub> formation was observed over the fresh catalyst but not the SO<sub>2</sub>-aged catalyst, which indicates that the fresh catalyst efficiently catalyzed steam reforming of CH<sub>4</sub> but was suppressed by sulfur poisoning. In these respects, the results of the NO-CH<sub>4</sub> reaction resemble those obtained under simulated exhaust conditions or in the NO-O<sub>2</sub>-CH<sub>4</sub> reaction.

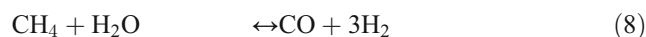
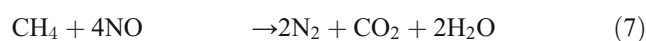
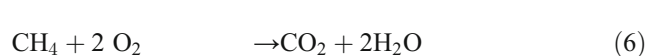
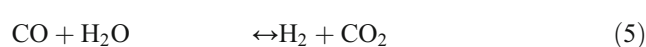
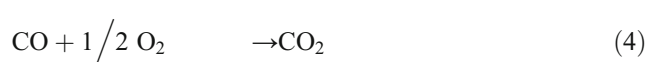
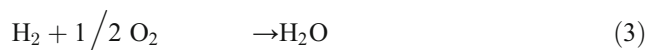
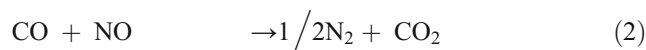
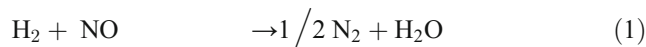
Figure 9 shows the N<sub>2</sub> yield from the NO-CH<sub>4</sub> reaction. Regardless of the reaction temperature and SO<sub>2</sub> aging, a high N<sub>2</sub> yield was obtained under stoichiometric conditions, but significant N<sub>2</sub>O formation was observed under lean conditions. N<sub>2</sub>O formation was observed at 400 and 450 °C after SO<sub>2</sub> aging. In particular, at 400 °C and λ=0.990, a large discrepancy was observed between the NO<sub>x</sub> conversion and the N<sub>2</sub>+N<sub>2</sub>O yield, suggesting that a significant amount of NH<sub>3</sub> was formed.

**Fig. 6** NO<sub>x</sub> and CH<sub>4</sub> conversions over Pt-Rh/CeO<sub>2</sub>-Al<sub>2</sub>O<sub>3</sub> in the NO-O<sub>2</sub>-CH<sub>4</sub> reaction. Reaction conditions: 2000 ppm NO, 1500 ppm CH<sub>4</sub>, 1000–4000 ppm O<sub>2</sub>, 11 % H<sub>2</sub>O



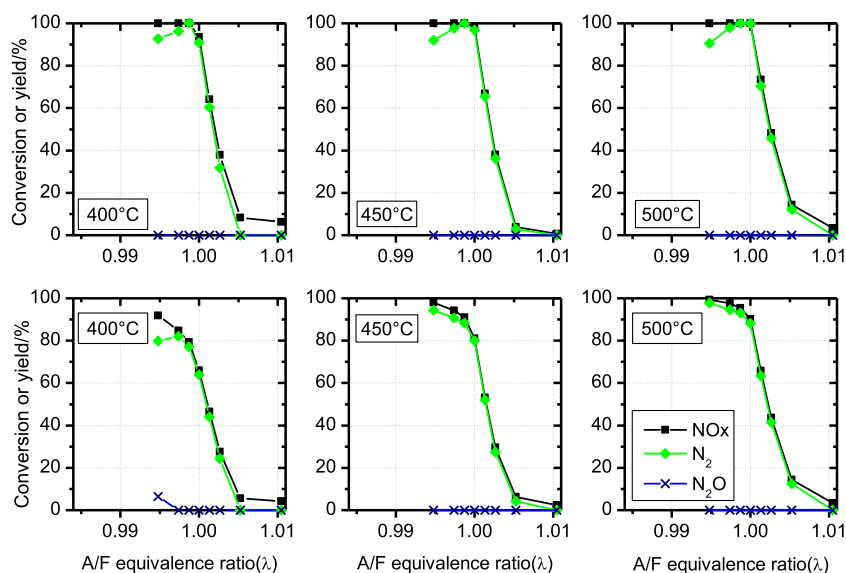
## 4 Discussion

Many reactions proceed simultaneously over three-way catalysts under conditions of actual emission control, and the chemistry of three-way catalysis is complicated [23]. When methane is the only the hydrocarbon species in the feedstream, as was investigated in this study, and only N<sub>2</sub> is considered as a product of NO<sub>x</sub> reduction, the following reactions contribute to exhaust purification:



Among these reactions, the reaction of NO (or O<sub>2</sub>) and CO (or H<sub>2</sub>) proceeds rapidly at temperatures of 300 °C or higher over noble metal catalysts. For example, Kobayakski and Taylor reported that NO reduction by H<sub>2</sub> over 0.5 wt% Pt/Al<sub>2</sub>O<sub>3</sub> gave 50 % conversion of NO at 121 °C and that NO

**Fig. 7**  $\text{NO}_x$  conversions and  $\text{N}_2$  and  $\text{N}_2\text{O}$  yields over Pt-Rh/CeO<sub>2</sub>-Al<sub>2</sub>O<sub>3</sub> in the  $\text{NO-O}_2\text{-CH}_4$  reaction before (upper column) and after (lower column) S aging. The reaction conditions were the same as in Fig. 6



reduction by CO over 0.5 wt% Rh/Al<sub>2</sub>O<sub>3</sub> gave 50 % conversion of NO at 296 °C [24]. Oh and coworkers investigated the CO-CH<sub>4</sub>-O<sub>2</sub> reaction over 0.2 wt% Pt/Al<sub>2</sub>O<sub>3</sub> and 0.14 wt% Rh/Al<sub>2</sub>O<sub>3</sub> catalysts. They observed complete conversion of CO at 200 °C over Pt/Al<sub>2</sub>O<sub>3</sub> and at 400 °C over Rh/Al<sub>2</sub>O<sub>3</sub> in an oxidizing feedstream and at 200 °C over both of Pt/Al<sub>2</sub>O<sub>3</sub> and Rh/Al<sub>2</sub>O<sub>3</sub> in a reducing feedstream [17]. By contrast, reactions involving CH<sub>4</sub> (reactions 6–8) proceed relatively slowly under the conditions used in this study (400–550 °C).

Steam reforming of CH<sub>4</sub> (8) is a highly endothermic reaction ( $\Delta H^\circ = 206$  kJ/mol) and is controlled by a thermodynamic equilibrium under typical conditions for H<sub>2</sub> production from CH<sub>4</sub>. However, under the conditions examined in this study (1500 ppm CH<sub>4</sub>, 11 % H<sub>2</sub>O, 6 % CO<sub>2</sub>, 400–550 °C), the equilibrium conversions of CH<sub>4</sub> are 99 % or higher, that is, the reaction is controlled by the reaction rate rather than the chemical equilibrium. The water-gas shift reaction (5) is a slightly exothermic reaction ( $\Delta H^\circ = -41$  kJ/mol) and is controlled by a chemical equilibrium with H<sub>2</sub>/CO ratios of ca. 6–20 under the conditions in this study (11 % H<sub>2</sub>O, 6 % CO<sub>2</sub>, 400–550 °C).

Therefore, in the three-way catalytic reaction under the conditions of gas engine exhaust at low temperatures, reactions of NO (or O<sub>2</sub>) and CO (or H<sub>2</sub>) are completed in an upstream part of the catalyst bed, and the overall conversion

is determined by reactions involving CH<sub>4</sub> (i.e., reactions 6–8) and the equilibrium-controlled water-gas shift reaction (5). Accordingly, the  $\text{NO}_x$  and CH<sub>4</sub> conversions under simulated exhaust conditions were in good agreement with those in the  $\text{NO-O}_2\text{-CH}_4$  reaction.

The methane conversion characteristics under the simulated exhaust conditions and in the  $\text{NO-O}_2\text{-CH}_4$  reaction were in good agreement with those in the O<sub>2</sub>-CH<sub>4</sub> reaction, and a large decrease with increasing  $\lambda$  under lean ( $\lambda > 1$ ) conditions was observed for all reactions. It is widely accepted that the CH<sub>4</sub> oxidation activities of Pt and Rh catalysts are maximal at approximately stoichiometric conditions and decrease under lean conditions due to strong adsorption of oxygen onto the active sites [17, 18].

The effects of SO<sub>2</sub> aging were small under lean conditions, but the  $\text{NO}_x$  and CH<sub>4</sub> conversions under stoichiometric conditions decreased remarkably at 450 °C and lower temperatures, while CH<sub>4</sub> conversion decreased drastically under rich conditions. Ansell and coworkers investigated the effects of SO<sub>2</sub> aging on the three-way catalytic reactions over Pt-Rh/CeO<sub>2</sub>-Al<sub>2</sub>O<sub>3</sub> in simulated exhaust containing CH<sub>4</sub> and C<sub>3</sub>H<sub>8</sub> [25]. They reported that CH<sub>4</sub> conversion under a lean condition of  $\lambda = 1.02$  slightly increased after SO<sub>2</sub> aging, while CH<sub>4</sub> conversion under a rich condition of  $\lambda = 0.98$  remarkably decreased after SO<sub>2</sub> aging. They concluded that the large

**Fig. 8**  $\text{NO}_x$  and CH<sub>4</sub> conversions over Pt-Rh/CeO<sub>2</sub>-Al<sub>2</sub>O<sub>3</sub> in the  $\text{NO-CH}_4$  reaction. Reaction conditions: 2000 ppm NO, 300–1500 ppm CH<sub>4</sub>, 11 % H<sub>2</sub>O

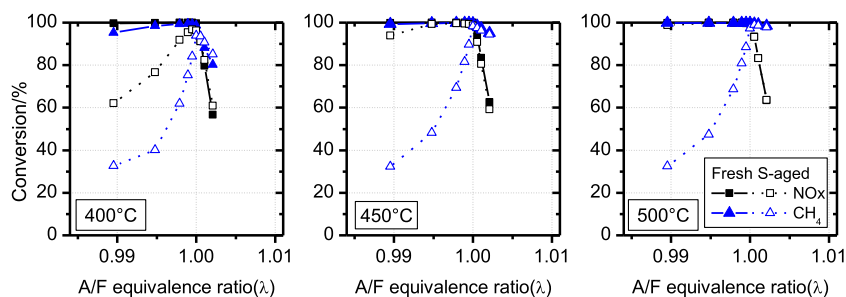
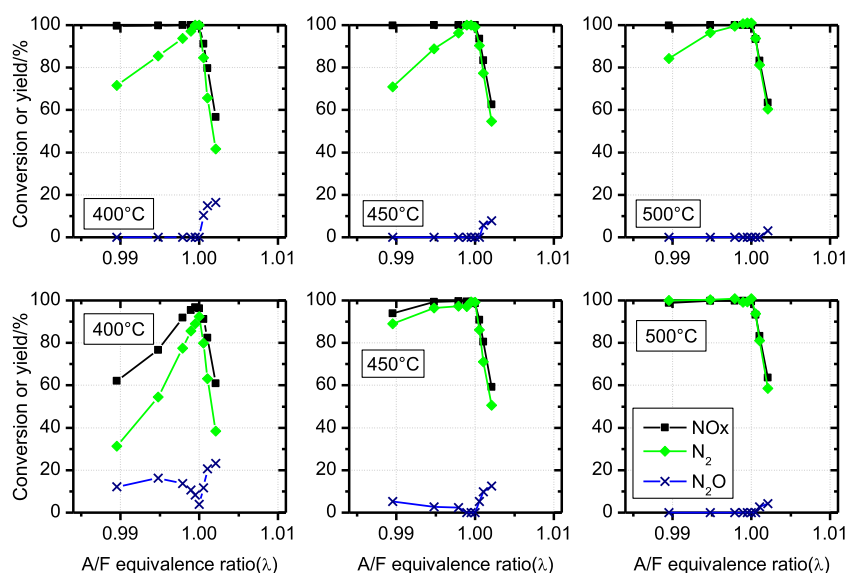


**Fig. 9**  $\text{NO}_x$  conversions and  $\text{N}_2$  and  $\text{N}_2\text{O}$  yields over Pt-Rh/CeO<sub>2</sub>-Al<sub>2</sub>O<sub>3</sub> in the NO-CH<sub>4</sub> reaction before (upper column) and after (lower column) S aging. The reaction conditions were the same as in Fig. 8



decrease in CH<sub>4</sub> conversion was caused by suppression of steam reforming due to sulfur poisoning. They also reported that the CH<sub>4</sub> conversion of the SO<sub>2</sub>-aged catalyst under rich conditions was maximal at 425 °C and decreased with increasing temperature up to 550 °C, in agreement with the results of the present study shown in Fig. 3. Taken together with the decrease in CH<sub>4</sub> conversion in the NO-O<sub>2</sub>-CH<sub>4</sub> reaction and the reaction under simulated exhaust as well as in the O<sub>2</sub>-CH<sub>4</sub> reaction, these results indicate that the decrease was caused by the suppression of steam reforming. The decrease in NO<sub>x</sub> and CH<sub>4</sub> conversions under stoichiometric conditions after SO<sub>2</sub> aging may be explained as follows. Over the fresh catalyst, in addition to the reaction path in which CH<sub>4</sub> reacts directly with O<sub>2</sub> and NO, another path exists in which CH<sub>4</sub> is converted to H<sub>2</sub> and CO via steam reforming, and the subsequent H<sub>2</sub> and CO react with O<sub>2</sub> and NO. Because the latter path is inhibited by sulfur poisoning, the reaction of CH<sub>4</sub> is limited to direct reactions with O<sub>2</sub> and NO, which leads to decreased activity.

By contrast, the NO<sub>x</sub> and CH<sub>4</sub> conversions under the simulated exhaust conditions and in the NO-O<sub>2</sub>-CH<sub>4</sub> reaction were strongly affected by SO<sub>2</sub> aging and were not sufficient at 450 °C or lower temperatures, and NO<sub>x</sub> and CH<sub>4</sub> conversions in the NO-CH<sub>4</sub> reaction at approximately stoichiometric conditions remained high even after SO<sub>2</sub> aging. The NO-CH<sub>4</sub> reaction over Pt/Al<sub>2</sub>O<sub>3</sub> has been investigated by Burch and Ramli [19, 20] and by Balint and coworkers [26], but these reports mainly focused on experiments under rich conditions, and catalytic activity under stoichiometric conditions and the differences between the NO-CH<sub>4</sub> and the NO-O<sub>2</sub>-CH<sub>4</sub> reactions remained unclear. The high NO<sub>x</sub> and CH<sub>4</sub> conversion in the NO-CH<sub>4</sub> reaction under stoichiometric conditions observed in the present study may be explained as follows. Under stoichiometric conditions in the NO-O<sub>2</sub>-CH<sub>4</sub> reaction,

O<sub>2</sub>, which is present at high concentrations, strongly adsorbs onto active sites and prevents the reaction of CH<sub>4</sub> and NO. In the NO-CH<sub>4</sub> reaction, the absence of O<sub>2</sub> increases the number of active sites available for reaction. If it is possible to increase activity by removing O<sub>2</sub> in the reactant, a combination of oxygen storage materials (e.g., CeO<sub>2</sub>) and suitable control of the air/fuel ratio may be effective for improving activity at lower temperatures. This effect may partly contribute to improved activity under periodic air/fuel control actually applied to automotive emission control systems [27–29]. However, an insignificant amount of N<sub>2</sub>O, which has a high global warming potential, was formed in the NO-CH<sub>4</sub> reaction at low temperatures under both rich and lean conditions. Suppression of N<sub>2</sub>O formation would be required to implement this strategy for improving low-temperature activity in practical applications.

## 5 Conclusions

This work demonstrates that Pt-Rh/CeO<sub>2</sub>-Al<sub>2</sub>O<sub>3</sub> exhibits sufficient three-way catalytic activity for controlling emissions from natural gas engines, even at 400 °C, in the absence of SO<sub>2</sub>. However, the catalyst is sensitive to sulfur poisoning, and its activity is insufficient at temperatures of 450 °C or lower. The decrease in activity is mainly due to suppression of steam reforming of CH<sub>4</sub>. Next-generation natural gas engines will have improved efficiencies, and the exhaust temperatures of these improved engines will be lower than those of current engines. Therefore, further catalyst improvements will be required to ensure low emissions from these improved engines, and the key issue will be to promote CH<sub>4</sub> conversion at low temperatures even in the presence of SO<sub>2</sub>.



**Acknowledgments** The author is indebted to Mr. A. Hirayama for adsorption measurements. The author thanks Mr. H. Fujita and Mr. M. Sako for their technical assistance with activity measurements.

## References

- Burnham, A., Han, J., Clark, C.E., Wang, M., Dunn, J.B., Palou-Rivera, I.: *Env. Sci. Tech.* **46**, 619 (2012)
- Tullo, A.H.: *Chem. Eng. News* **87**(38), 26 (2009)
- Whitney, K.A., Bailey, B.K.: SAE 941903 (1994)
- Da Costa, P., Salaün, M., Djéga-Mariadassou, G., Da Costa, S., Brecq, G.: SAE 2007-01-0039 (2007)
- Salaün, M., Kouakou, A., Da Costa, S., Da Costa, P.: *Appl. Catal. B.* **88**, 386 (2009)
- Matam, S.K., Otal, E.H., Aguirre, M.H., Winkler, A., Ulrich, A.: *Catal. Today* **184**, 237 (2012)
- Tabata, T., Baba, K., Kawashima, H., Kitade, K., Tanaka, T., Kokitsu, M., Ohtsuka, H., Okada, O.: *Stud. Surf. Sci. Catal.* **92**, 453 (1995)
- Tabata, T., Baba, K., Kawashima, H.: *Appl. Catal. B.* **7**, 19 (1995)
- Tabata, T., Kawashima, H., Baba, K.: *Stud. Surf. Sci. Catal.* **111**, 259 (1997)
- Nishizaka, Y., Misono, M.: *Chem. Lett.* **22**, 1295 (1993)
- Loughran, C.J., Resasco, D.E.: *Appl. Catal. B.* **7**, 113 (1995)
- Ohtsuka, H., Tabata, T., Hirano, T.: *Appl. Catal. B.* **28**, L73 (2000)
- Ohtsuka, H.: *Catal. Lett.* **87**, 179 (2003)
- Mirkelamoglu, B., Ozkan, U.S.: *Appl. Catal. B.* **96**, 421 (2010)
- Gawade, P., Alexander, A.M.C., Silver, R., Ozkan, U.S.: *Energy Fuels* **26**, 7084 (2012)
- Subramanian, S., Kudla, R.J., Chattha, M.S.: *Ind. Eng. Chem. Res.* **31**, 2460 (1992)
- Oh, S.H., Mitchell, P.J., Siewert, R.M.: *J. Catal.* **132**, 287 (1991)
- Oh, S.H., Mitchell, P.J., Siewert, R.M.: In: Silver, R.G., Sawyer, J.E., Summers, J.C. (eds.) *Catalytic control of air pollution*, p. 12. American Chemical Society, Washington, D.C. (1992)
- Burch, R., Ramli, A.: *Appl. Catal. B.* **15**, 49 (1998)
- Burch, R., Ramli, A.: *Appl. Catal. B.* **15**, 63 (1998)
- González-Velasco, J.R., Botas, J.A., González-Marcos, J.A., Gutiérrez-Ortiz, M.A.: *Appl. Catal. B.* **12**, 61 (1997)
- Shelef, M., Gandhi, H.S.: *Ind. Eng. Chem. Prod. Res. Develop.* **11**, 393 (1972)
- Taylor, K.C.: In: Anderson, J.R., Boudart, M. (eds.) *Catalysis, science and technology*, vol. 5, p. 119. Springer, Berlin (1984)
- Kobylinski, T.P., Taylor, B.W.: *J. Catal.* **33**, 376 (1974)
- Ansell, G.P., Golunski, S.E., Hatcher, H.A., Rajaram, R.R.: *Catal. Lett.* **11**, 183 (1991)
- Balint, I., Miyazaki, A., Aika, K.: *Appl. Catal. B.* **37**, 217 (2002)
- Muraki, H., Shinjoh, H., Sobukawa, H., Yokoya, K., Fujitani, Y.: *Ind. Eng. Chem. Prod. Res. Dev.* **24**, 43 (1985)
- Muraki, H., Fujitani, Y.: *Ind. Eng. Chem. Prod. Res. Dev.* **25**, 414 (1986)
- Shinjoh, H., Muraki, H., Fujitani, Y.: *Appl. Catal.* **49**, 195 (1989)